Digest of Translated Russian Literature

The following abstracts have been selected by the Editor from translated Russian journals supplied by the indicated societies and organizations, whose cooperation is gratefully acknowledged. Information concerning subscriptions to the publications may be obtained from these societies and organizations. Note: Volumes and numbers given are those of the English translations, not of the original Russian.

RADIO ENGINEERING AND ELECTRONIC PHYSICS (Radiotekhnika i Elektronika). Published by American Institute of Electrical Engineers in conjunction with Scripta Technica, Inc., New York

Number 1, January 1962

Effectiveness of a System Composed of a Frequency Filter and a Delayed Feedback Storage Unit, Yu. S. Lezin, pp. 34–39.

The improvement in the signal-to-noise ratio guaranteed by the combination of a frequency filter with a storage unit with delayed feedback, in comparison with an optimal filter for a single pulse signal, is calculated. The choice of the bandwidth of the prestoring filter, as well as of the filter in the feedback loop of the storage unit, are examined.

Conclusions: The peak value of the signal and the power of the noise at the output of the system comprised of a frequency filter and of a storage system with delayed feedback are determined. The gain in the signal-to-noise ratio guaranteed by the given system is calculated in comparison with the one obtained in an optimal filter for a single pulse signal. Results of calculations are presented graphically, which permits easy determination of the magnitude of gain for various parameters of the filter and of the storage unit.

It is shown that, in order to obtain a large gain, the bandwidth of the filter which is connected in the feedback loop of the storing unit must be broadened, and the bandwidth of the prestorage filter must be chosen optimally. When the bandwidth of the filter in the feedback loop of the storage unit is sufficiently large and when the bandwidth of the prestorage filter is optimal the gain increases as the feedback coefficient approaches unity, and for $m = 0.08$–0.95 is in the order of 7–37. In comparison with the case when both filters are identical and their bandwidths are chosen optimally, the indicated gain is 3–6 times greater.

If for some reason one cannot sufficiently widen the bandwidth of the filter in the feedback loop of the storing unit, then by narrowing several times the bandwidth of the prestorage filter, one may increase the signal-to-noise ratio at the output by as much as a factor of 2.

Variational Method for the Calculation of Parameters Which Are Linear Functionals of the Electrodynamic Integral Equations, Ya. N. Fel'd, pp. 46–53.

A general method is presented for the construction of functionals which are stationary for those functions which coincide with the solution of the given linear operational equation. The stationary values of these functionals may be made equal to any arbitrary parameter which is a linear function of the solution of the operational equation. The method is equally applicable to equations with symmetrical and nonsymmetrical operations and can be used for the approximate calculation of different parameters. As an example, the author presents a stationary expression for the directivity pattern of cylindrical antennas.

Synthesis of Stepped Transition Units with Maximally Flat Frequency Characteristics, L. R. Yavich, pp. 93–100.

A method is suggested for computing the characteristic impedances of stepped transition units for any desired number of steps. The numerical values for $n = 4$, 5, and 6 are tabulated. The possibilities of computing the characteristic impedances of steps, using the theory of first approximation, are discussed.

Transition units with maximally flat frequency response enjoy definite advantages over the Chebyshev type, although they are inferior to the latter in terms of passband, all other conditions being equal. Significant advantages enjoyed by these types of transition units are the constancy of the in-phase component and the small quadrature component of the input impedance.

In another paper examination was made of the synthesis of stepped transition units with a maximally flat frequency-response curve by the method of indeterminate coefficients. The cumbersome nature of the expressions made it possible to determine a relationship between the characteristic impedances of the steps only for two- and three-step transition units ($n = 2, 3$). The present study has made use of the classical method of synthesis generalized to the case of links (circuits) with distributed constants. This approach to the problem permits rather simple computation of the parameters of transition units with any number of steps n which have the required frequency-response curves.

Dynamic Programming Applied to Recording Weak Signal Levels by Inertial Dynamic Systems in the Presence of Noises, Yu. B. Sindler, pp. 142–145.

This note considers the problem arising in automatic recording of the level of weak signals by means of inertial dynamic systems such as inertial automatic recording devices.

Number 2, February 1962

Sampling of a Variable Frequency Signal from the Background Noise, R. L. Stratonovich, pp. 171–178.

For the optimum sampling of a narrowband signal having an unknown frequency from the background noise, the present paper proposes a method that employs coupled parallel circuits, adapted to operate under conditions of constant or variable signal parameters, as well as with regular or random frequency changes.

A paper dealing with the sampling of a narrowband signal of unknown frequency in a background of noise, proposes a method based on the principle according to which the resonance frequency of a tuned circuit follows the estimated frequency of a signal. The optimum circuit described in the reference involves certain difficulties, however, since little initial data concerning the frequency of the signal is available. In order to overcome these difficulties it is advantageous to employ another filtering principle, namely, the principle according to which a plurality of circuits tuned to different frequencies operate simultaneously.

In the simplest form, the circuits are uncoupled. A receiving system under this condition is discussed elsewhere. According to theory, a system of uncoupled circuits may be considered optimum if the real frequency of the signal, though unknown, is a priori constant. In the case of a variable frequency, the optimum case is obtained with a system of coupled circuits. The parameters of the individual circuits and their degree and form of coupling will be calculated in the present article, using optimum nonlinear filtering theory and Markov processes.

Scattering of Fluctuating Waves by Objects of Large Dimensions, Ye. A. Shtager, pp. 185–189.

The present article discusses the application of Kirchhoff's method to the problem of scattering of fluctuating waves by bodies of various geometrical shapes. As an example, a problem in the scattering of fluctuating waves by a rectangular plate is solved, and a comparison is presented between the resulting averaged reflection pattern and the reflection pattern with the plate in a uniform or homogeneous field.

An analysis of the diffraction and scattering phenomena of fluctuating waves (waves that are nonuniform in the incident field) brings to light interesting properties. It is of practical interest to know whether it is necessary to calculate the reflection patterns from the different bodies placed in the fluctuating field, since in real conditions the field is usually subject to disturbances.

A discussion of several questions connected with the scattering of fluctuating waves is given. It is assumed that the random amplitude and phase changes are stationary processes and that these changes occur slowly enough that the reflection process may be considered to be in a steady state.

Diffraction of Radio Waves around the Earth through Inhomogeneous Atmospheric Layers, N. A. Armand, pp. 206–212.

We will examine the effect of nonlinear altitude profiles of the specific inductive capacitances of air during diffraction of ultrashort waves at the earth's surface. The problem is analyzed by the method of reference equations. It will be shown that the result depends on the magnitude of the so-called "Schwarz derivative." When the magnitude of this derivative is small, the effect of nonlinearity of the altitude profile of the specific inductive capacitance results in slight adjustments in the magnitude of the equivalent radius of the earth.

Conclusion: The foregoing discussion leads to the conclusion that the notion of equivalent radius of the earth is applicable even in the case of a nonlinear but sufficiently smooth altitude profile of the index of refraction of air. The adjustments which arise in this case [because of the nonlinearity of the profile of $n(h)$] can be considered insignificant.

The value of the Schwarz derivative can serve as a criterion for smoothness or "roughness" on the profile of $n(h)$. In any case, it follows from a given formula that the Schwarz derivative must be large wherever there is a discontinuity in either $n(h)$ or dn/dh. Because of this, the Carroll and Ring model does not satisfy the condition of smoothness, since, at the point $h = H$, $r(y)$ is converted to a delta-function, and the Schwarz derivative is infinite. From this point of view, the Carroll and Ring model does not reflect the averaged properties of the troposphere and is artificial.

However, in this connection the question arises of what will happen in those cases where, at certain altitudes, $n(h)$ changes in magnitude as rapidly as the Schwarz derivative and cannot be neglected. Obviously, in these cases the problem changes qualitatively and requires different methods for its solution.

Correlation of Amplitude and Phase Fluctuations of Radio Waves Propagated in the Troposphere, A. V. Men', pp. 215–221.

We will investigate the correlation between amplitude and phase fluctuations at the same point in space, which arise during propagation of waves about a flat interface in an inhomogeneous turbulent medium. It will be shown that the theoretical results concerning the lack of correlation of these fluctuations in a distant region, which Chernov obtained under the assumption of an unlimited medium, hold also for the present case. We will introduce results of experimental measurements of the correlation of amplitude and phase fluctuations during propagation in lower tropospheric layers in both the illuminated region and the region obscured by the curvature of the earth's surface.

Method of Nonself-Adjoint Operators in the Theory of Waveguides, M. S. Livshits, pp. 260–276.

The present paper is devoted to the application of a recently developed spectral theory of nonself-adjoint operators to the subject of the propagation of waves in waveguides. The triangular model of operators is particularly convenient for this purpose. By applying the theory of nonself-adjoint operators, one may obtain solutions of a wide class of both stationary and nonstationary problems for nonuniform waveguides, as well as for waveguides and cavity resonators with branches. The solutions are in the form of a series in certain orthogonal "model" fields, which have a simple physical meaning: the model fields are generalized concepts of the principal vibrations in a closed system. It is known that many important problems in the theory of waveguides were solved by the method of expansion in eigenfunctions of various self-adjoint boundary problems. Thus, one must usually solve a system of an infinite number of linear equations, so that it is quite difficult to obtain a final result and difficult to study. In this paper there also emerges a system of linear equations, easily solved by application of the triangular model.

The general properties of a scattering matrix were investigated in another paper, and its use in the theory of cavity resonators was demonstrated. In this way we obtained, by simple means, results of practical interest, but the field inside the cavity resonator remains unknown. The question arises: how can information concerning the field inside the cavity resonator (or any nonuniformity) be obtained by using the scattering matrix? It is shown below that after determining the dependence of the scattering matrix on the frequency ω, one may find the Fourier coefficients of the unknown field in an expansion with respect to the model fields and the contribution of individual fields to the total field, completing the solution of Maxwell's equation. When necessary, the model fields can be calculated by any degree of accuracy from the solution of a certain nonself-adjoint boundary problem for Maxwell's equations. The theory of triangular models and its application to the quantum mechanical problem of scattering is contained in other papers, but knowledge of these papers is not a prerequisite for an understanding of the present paper.

Sensitivity of Quantum Electromagnetic Radiation Receivers, N. V. Karlov and A M. Prokhorov, pp. 305–315.

The sensitivity of quantum amplifiers and counters is examined.

Operating Characteristics of Transistorized Integrating Operational Amplifiers, V. T. Frolkin, pp. 316–319.

Transistorized integrating operational amplifiers are analyzed on the basis of current control of these devices. The derived relationships permit evaluation of the efficiency of various amplifier circuits and rational choice of the principal parameters.

Fig. 1 Generalized block diagram of transistorized integrating operational amplifier.

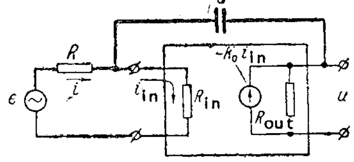

Analysis of the operation of transistorized integrating operational amplifiers with feedback as performed by the procedure adopted for vacuum-tube amplifiers does not give a complete picture of the specific aspects of transistor circuits, which makes practice difficult and in some cases, as is shown, may lead to incorrect conclusions. The chief characteristic of the transistor is the fact that it is a current-controlled device, as a result of which the current gain is regarded as the principal parameter while the voltage gain is considered derivative. The generalized block diagram of a transistorized integrating operational amplifier is given in Fig. 1 and is used in the ensuing analysis. In this diagram, parameters R_{in}, R_{out}, and K_0 are, respectively, the input and output resistances and the current gain of an amplifier without feedback.

Number 3, March 1962

Linear Coding of Images, B. S. Tsybakov, pp. 351–361.

Possibilities using two-dimensional space filtering for coding and decoding of images are described. An idealized two-dimensional communication channel is designed which can reasonably be examined in connection with the transmission of stationary images. The optimal characteristics of two-dimensional coding and decoding filters are calculated, and the mean square error corresponding to them is found. An example of an isotropic image with an exponential correlation function is examined.

Conclusions:

1) It is expedient to accomplish the coding of two-dimensional information before it is scanned. In this way coding of the entire image can be accomplished as a whole, whereas coding performed after scanning can encompass only points of the image which are near each other along a scan line.

2) Coding which allows for the probability characteristics only along a line (one-dimensional coding) is never better than coding which allows for these characteristics throughout the plane of the image. It can be shown, for example, that for the case examined in Sect. 3, one-dimensional coding does not improve transmission quality.

3) The discussions conducted here can be generalized for the case of transmission of information which is a function of an arbitrary number of variables. Thus, for example, in television the use of three-dimensional coding and decoding may be of significant value.

Theory of Resonant Ferrite Systems, Hsü Yen-shêng, pp. 403–411.

The report investigates the resonance conditions of transversely magnetized round and elliptical rods within a rectangular waveguide by the method of successive approximations. Influence of the waveguide wall is taken into account by the method of images. Various resonance conditions for the forward and backward waves of the waveguide are derived.

Conclusions:

1) The difference in the resonance fields for the forward and backward waves is due chiefly to the influence of the TE_0 wave within the rod, the field of which decreases slowly with increasing distance from the rod, and hence the influence of the wall on it is more significant.

2) Theoretical explanation has been given for the following effects: a) the value of the resonance field for the backward wave is greater than for the forward wave; b) a ferrite slab in the H-plane results in a greater difference in resonance fields than in the E-plane.

3) A circular rod or extremely thin slab is not suitable for use as an isolator, for in these cases the difference in resonance fields of the forward and backward waves is extremely small, as the foregoing analysis shows.

4) For the case of rods in which $a \simeq b$, calculation with the derived approximate formula yields a considerably smaller difference in resonance fields than does experiment. In order to obtain agreement of theoretical and experimental results, a rigorous solution of the problem of a rectangular rod is required, which is extremely difficult.

Frequency Stabilization of Reflex Klystron by Means of Auxiliary Cavity, G. M. Utkin and A. V. Khryunov, pp. 421–432.

The report discusses a reflex klystron in which, for frequency stabilization, the main cavity is coupled with an auxiliary high-Q cavity. Two variants of the system are discussed: 1) the load is fed from the main cavity; 2) the load is fed from the auxiliary cavity. Power to load, klystron frequency, and frequency stability are given as functions of various parameters, permitting the calculation of optimum operating conditions for the system. It is shown that the first variant of the system permits higher stability factor, higher power to load, and greater electronic tuning range by use of the auxiliary cavity than the second variant.

Amplitude Distribution of Photomultiplier Output Current Pulses, N. S. Khlebnikov, A. Ye. Melamid, and T. A. Kovaleva, pp. 488–494.

The report describes a procedure for measuring the amplitude distribution of output pulses of a photomultiplier (FEU) created by individual electrons at the output of a dynode system and presents the results of experiment. The change in distribution conditions is determined as a function of the operating conditions of the FEU. With proper choice of multiplier and operating conditions the amplitude distribution is similar to a Poisson distribution.

Conclusions:

1) It is established that the amplitude distribution of output pulses of a photomultiplier when individual electrons appear at the multiplier input is similar to a Poisson distribution.

2) This experimental fact supports the conclusions presented in another paper.

3) Detection of such distribution in experiment is possible only by means of photomultipliers having a plateau on the count-rate characteristic and operating under the plateau conditions.

4) Distribution of amplitudes with supply voltages lower than those which correspond to the plateau is exponential with a single slope; the distribution at voltages greater than those which correspond to the plateau has two maxima.

5) The exponential amplitude distribution of output pulses of a photomultiplier as observed by a number of authors may be due to the fact that either the multiplier was investigated under conditions which were unsuitable for these purposes or the discharge phenomena in the multiplier occurred before the gain of the system was sufficient to make possible the recording of each electron incident at the first dynode.

6) Contrary to the data presented by Zavoyskiy, Butslov, and Smolkin, the dark-current pulses of antimony-cesium photocathodes represent the emission of individual electrons and not of groups of electrons.

Theory of the Phototriode, Yu. I. Ravich, pp. 494–503.

The current of a phototriode was calculated for the case of an arbitrary voltage and for constant or sine-modulated illumination of the emitter, the collector and the base regions. The influence of the accelerating field in base and emitter, of surface recombination, of contact resistance and junction leakage, of carrier generation and recombination in p-n junctions, and of a high injection level in the base was considered.

Conclusions:

1) An expression has been obtained by solving diffusion equations for the total current for any voltage and nonuniform illumination of emitter, collector, and base. It was shown that the photocurrent in a phototriode, connected in a circuit with an open base, is equal to the current of photocarriers, separated by the p-n junctions, multiplied by the current amplification coefficient of a transistor in a common emitter (or common collector) circuit.

2) The photocurrent is found to be proportional to the total number of photocarriers separated by the junctions. It is therefore unimportant as a matter of principle and from the viewpoint of providing a high effective quantum yield, which region, emitter, collector, or base is subjected to radiation.

3) In presence of a small series resistance of the emitter and collector regions the current grows fast with an increase of the voltage applied to the phototriode, reaching saturation at voltages exceeding several kT/q. Here, the collector voltage can be forward biased.

Number 4, April 1962

Reflection of Radio Waves by Inclined Meteorite Trails, M. D. Khaskind, pp. 558–567.

The field of scattered waves when plane electromagnetic waves are incident to an ionized meteorite trail at an arbitrary angle with respect to its axis is analyzed. A microwave approximation is based on the method of polarization currents for trails having an arbitrarily smooth structure. A long-wave approximation is evaluated at large linear electron concentrations in the trails. The complete solution is obtained using special electromagnetic potentials of axially symmetrical plasma, for which a system of simultaneous equations is derived. The article analyzes the limiting properties of these potentials.

Two-Sided Approach to the Determination of the Natural Frequencies of Cavity Resonators Containing Heterogeneous Anisotropic Media, V. V. Nikol'skiy, pp. 567–581.

A method is developed for the solution of electrodynamic problems by a two-sided determination of eigenvalues. The method employs the principle of comparison of operators, similar to the method of Svirskiy. A simple method for finding the natural frequencies of electromagnetic cavity resonators containing heterogeneous (isotropic and anisotropic) media is given. A method for evaluation of errors and examples are cited.

Conclusions:

1) The basic conclusion is that the method given for a two-sided determination is a very simple means for computing irregular resonators (see the examples given in the supplement). The accuracy of the results for the simplest variant is adequate for most technical applications; theoretically the accuracy can be infinitely improved. It is interesting to note that in the case of an electrical disturbance (dielectric bodies in a resonator), it is easy to construct a universal table for computing resonant frequencies, the parameters of which will be the quantities q, ϵ, and β_2/B_1 (the latter is the square of the ratio of the first two natural frequencies of cavity systems. These quantities completely locate both limits of the lowest natural frequency regardless of the type of irregularity. In using the tables, when calculating resonators of arbitrary types, it is only necessary to know or calculate beforehand the form factor q.

Table 4

$\sqrt{10}\frac{\omega_1}{\omega_0}$, mean	$\sqrt{10}\frac{\omega_1}{\omega_0}$, accuracy	Error, %	$\sqrt{10}\frac{\omega_1}{\omega_0}$, mean	$\sqrt{10}\frac{\omega_1}{\omega_0}$, accuracy	Error, %
2.53	2.605	−2.9	1.078	1.082	−0.37
1.92	1.915	+0.26	1.038	1.031	+0.68
1.53	1.495	−2.34	1.013	1.011	+0.20
1.30	1.285	+1.17	1.0025	1.0015	+0.10
1.16	1.160	0.00	1.0000	1.0000	0.00

2) The function f_1 was selected in this paper as a normalized basic field. Such a method has the advantage of simplicity, yet it is not entirely preferable. The choice of f_1 (see Sec. 3) can result in an increase of the lower limit. Strictly speaking, a lowering of the upper limit can be accomplished by the specific selection of the test function in functionals.

3) Theoretically we can calculate not only the lowest but also other natural frequencies.

4) We can develop a waveguide method from the resonator method. In the direct transition, complete information on the waveguide will be obtained from the natural frequency of a waveguide resonator. In all complex cases (for nonreciprocal types), the critical frequency of the waveguide can be determined. Apparently, we can construct a special waveguide procedure using different operators.

5) The two-sided method of calculation also permits the determination of the accuracy of the different types of approximations in the theory of disturbances. It is essential that the zero approximation for a formula in another paper give results of the same type as those for the upper limit in the examples considered here.

6) In all examples only small errors in the mean results were found. In reality the results can be significantly more accurate. This is illustrated in Table 4, where it is possible to compare the results in example 3 with the computer results up to the 20th harmonic which are here rounded off to 4 or 5 significant figures and labeled "accurate" (for the principle of calculation see a reference given; computations were performed by V. G. Sukhov on the computer "Strela" (Arrow).

Contribution to the Theory of Diffusion Waves in a Plasma, Stationary in a Longitudinal Magnetic Field, V. S. Golubev and V. L. Granovskiy, pp. 624–630.

A theory of diffusion waves, propagating in a gas, located in a longitudinal magnetic field, is developed for a periodically varying concentration of charge carriers in the initial portion of the gas volume. The dependence of the wave number and the attenuation of the diffusion wave on the magnetic field intensity and other conditions is investigated. The observation of such waves can permit the determination, through new methods, of the coefficient of transverse diffusion of charge carriers in a gas located in a magnetic field.

Determination of Antenna Length for a Given Radiation Pattern, V. I. Popovkin, pp. 662–666.

1. Complex Multiplier of a System of Radiators

We will define a linear antenna as a combination of identically polarized, monochromatic sources of an electromagnetic field, distributed either continuously or discretely in a region at points whose distance from the system axis are small as compared to the wavelength. A linear antenna is characterized by the scalar function $J(x)$, that is, by either $E(x)$ or $H(x)$, which describes the continuous (discrete) distribution of amplitudes and phase currents (fields) averaged at each point x along its transverse cross section.

The problem of the synthesis of a linear antenna can be divided into two problems: the first consists of finding, for a given directivity pattern, the shortest antenna length for which the problem is solvable. The second problem is the determination of the physically attainable discrete or continuous current (field) distributions along the antenna axis of known length which will permit the given complex directivity pattern to be obtained either precisely or approximately.

The first synthesis problem apparently has been little investigated. The second problem has been studied in a number of works in which various methods for its solution have been proposed. These latter methods all assume that, besides the radiation pattern, the antenna length is also given. In this paper the problem is posed in the following manner: it is required to determine the class of radiation pattern which permits an exact synthesis for a limited variation of the distribution function of the sources, and the antenna length corresponding to a given pattern in this class.

Conclusions:

1) Only integral functions of finite degree limited to the real axis can serve as complex multipliers of a linear system of radiators.

2) The electrical length of an antenna can be found independently of distribution of the sources. It is determined by the growth of the given finite-degree integral function in the direction of the imaginary axis: $2a = 2h(\pi/2)$. The antenna length can also be determined by the density of the roots of this function on the real axis:

$$2a = 2\pi \lim_{n\to\infty} \frac{n}{\alpha_n}$$

Number 5, May 1962

Investigation of the Frequency Tuning of a Molecular Oscillator by Modulating the Emission Line with the Aid of an External Magnetic Field, V. V. Nikitin and A. N. Orayevskiy, pp. 814–820.

The frequency tuning of a molecular oscillator with the aid of an external magnetic field has been investigated theoretically and experimentally. It has been shown that the presence of a magnetic hyperfine structure with different coupling constants at the upper and lower inversion levels leads to a shift in frequency of a molecular oscillator, tuned by a varying magnetic field, with respect to the frequency of a molecular oscillator, tuned by varying the pressure. The relative difference of the magnetic interaction constants has been established for the $J = 3$, $K = 2$ $N^{14}H_3$ line for the upper and lower inversion levels.

Efficiency of Various Pumping Systems in Ruby Traveling-Wave Masers, V. B. Shteinshleiger, G. S. Misezhnikov, and O. A. Afanas'yev, pp. 828–833.

A comparison is made between three possible working systems of quantum-mechanical paramagnetic ruby amplifiers and using a different quantum transition for amplifiers and using a different quantum transition for pumping. The dependence of the amplification coefficient of traveling-wave quantum mechanical paramagnetic amplifiers on chromium concentration and temperature was investigated in these systems.

Conclusions: Several pumping modes are possible in a traveling-wave quantum-mechanical paramagnetic ruby amplifier with an orientation of the magnetic field normal to the crystal axis, using for amplification in the centimeter wave range the 1–2 transition, whereby the pumping power saturates either the transition 1–3, or 1–4, or finally the transitions 1–3 and 3–4 simultaneously. The value of the active magnetic decrement of the substance is, under otherwise equal conditions, several times larger in the mode with the saturation of the 1–4 transition than in the mode using the transition 1–3 for pumping.

The traveling-wave quantum-mechanical paramagnetic amplifier can therefore work in the first case at a considerably higher temperature than in the second case. The efficiency of such an amplifier strongly depends on the chromium ion concentration which has an optimum value c. It is shown that experimentally obtained values for the inversion coefficient of pumping modes ν_{14} and $\nu_{13} + \nu_{34}$ are close to values calculated on the basis of the theory of spin-lattice relaxation for a small concentration of paramagnetic ions.

Maser Radiation Line Width, V. S. Zuyev and I. V. Cheremiskin, pp. 869–870.

In studying the frequency stability of a maser a question arises with regard to the radiation line width and its dependence on the molecular beam intensity. There is also interest in the line width dependence on the molecular beam source structure (thin diaphragm, long channel). At low beam intensities the maser bandpass coincides with the spectral line width, but its observation and measurement is difficult because of a low receiver sensitivity. At higher beam intensities the bandpass narrows down considerably due to regeneration, and its direct measurement does not reflect the spectral line width. To measure the line width it is convenient to use the following method. Having determined how the bandpass depends on a selfexcitation parameter over the range of beam intensities, where observation is not limited by the receiver sensitivity, one can extrapolate the obtained curve toward the zero beam intensity thus getting the initial bandpass.

The maser bandpass α_0 depends on τ, the mean time it takes a molecule to traverse the resonator, and the self-excitation parameter β as follows:

$$\alpha_0 = 2[(1 - \beta)/\tau \quad (1)$$

This relationship was obtained from the power amplification coefficient

$$k = \frac{[(1/\tau^2) + \alpha^2]^2}{[\alpha^2 + (1/\tau^2)(1 - \beta)]^2} \quad (2)$$

Here α is detuning with regard to the line center frequency. Expression (2) follows from the theory worked out in another paper under assumptions that the line quality factor exceeds that of the resonator that detuning is not more than a few line widths, and that there is no saturation.

The mean flight time τ depends on the molecular velocity distribution. This distribution does not remain constant but varies somewhat with changes in the selector voltage, and the foregoing linear dependence of α_0 on β will be upset. This effect was noted in a reference given where variations in the velocity distribution of the selected molecules were evaluated from the maser frequency vs selector voltage curves. In this work derivations are given which explain satisfactorily the experimentally obtained curves. The magnitude β can be easily obtained experimentally if the maximum gain coefficient k_{max} is measured (at $\alpha = 0$). From (2) follows

$$k_{max} = \frac{1}{(1 - \beta)^2} \quad (3)$$

Measurements were conducted on a maser with an ND_3 beam and with an NH_3 beam. For a "net" type beam source 0.05 mm thick and with 0.05×0.05 mm opening the ND_3 line width turned out to be 800 cps (at the source temperature of 300°K and a resonator length of 40 cm) which is twice wider than the theoretical width, and for NH_3-5 kc (at $T = 3000$°K and a resonator length of 80 mm) which is 2.5 times wider than the theoretical width. Both in ND_3 and NH_3 a linear behavior of narrowing bandpass was observed during regeneration. For ND_3 narrowing was investigated from 750 to 20 cps, for NH_3—from 4.5 kc to 100 cps. We never observed any deviation from linearity. The measurement accuracy was on the order of 15%. In the case of ND_3 the accuracy was limited by the resonator frequency stability which was not thermostatically controlled, and in the case of NH_3 by receiver sensitivity (for ND_3 a synchronous detection was employed).

The line width increase can be partially ascribed to an indeterminate superthin structure (30%) and the remainder to the Doppler effect which evidently appears as a consequence of the field distortion by the partition waveguides and the beam divergence.

Measurements showed that the line width in the beam formed by a canal with a larger opening (2 mm in diameter and 10 mm long) significantly increases (by a factor of 2) only at beam source pressures which yields maximum output power.

Radiation line observations were made with a superheterodyne receiver. A quartz multiplier was used as a monochromatic source. Low frequencies were obtained by mixing a low frequency signal with the input signal. The maser served as a spectrum analyzer.

Number 6, June 1962

Longitudinal Photocell for Large Illuminations, T. Ya. Gorbach and K. M. Krolevets, pp. 995–998.

A nonuniform front illumination of an electron-hole junction leads to the appearance of a potential gradient with a component parallel to the plane of the junction. This was first noticed elsewhere for a particular case, and a practical application of this "longitudinal photo-effect" was also proposed in it for a direct measurement of a position change of a light beam in space. A number of properties of such "longitudinal photocells" for recording displacements were examined in other papers. A general analysis of phenomena for nonuniform illumination was made in another paper where, however, the solution of the basic equation of the longitudinal photoeffect was obtained only for small illuminations (in any point the transverse potential difference of a p-n junction $V \ll kT/q$) for the case of sharp light-dark boundaries. The case of sharp light-dark boundaries at any illumination was discussed in detail in references given where a "saturation" with a rise in illumination of the transverse potential difference was discovered in the unilluminated parts of the junction. This circumstance can be used in the longitudinal photocell to eliminate the dependence of its readings on illumination.

Number 7, July 1962

Storage in Camera Tubes with Photoconductive Targets, S. P. Zelenoborskiy, pp. 1110–1119.

The report discusses problems of charge image storage on high-resistance photoconductive targets; an evaluation of fluctuations is given in the presence of storage of charge image in a vidicon.

Conclusions: The storage current of camera tubes with photoconductive targets may be represented as the product of the photocurrent of storage of the corresponding photoemissive camera tube and the internal photoconductive gain G. Internal gain is accompanied by the same low noise as in the case of secondary-electron amplification. Thermal fluctuations in the target element are small in comparison with fluctuations in the stored charge, which permits disregarding of these fluctuations in estimating the signal-to-noise ratio of the stored charge of the target.

Fluctuations in the stored charge of a target element are determined chiefly by fluctuations in the storage carriers generated by the luminous flux. On this basis we may regard the storage of the charge pattern in a vidicon as a practically ideal conversion of luminous flux into electric charges. In the process of commutation of the charge pattern of the target, the signal-to-noise ratio is additionally degraded, but this deterioration in the presence of optimum selection of the dark resistance of the target is negligible. The high signal-to-noise ratios which may be obtained in practice in vidicons support the conclusions given in this report.

Values of internal gain G, in distinction from secondary-electron emission, may reach values of the order of hundreds and even thousands. The mentioned values of G are achieved in photoconductive cells of cadmium sulfide manufactured by a special process. Unfortunately, sensitive photocells of CdS have a dark conductivity several orders of magnitude greater than required for vidicon layers.

Simple calculation shows that the required value of G for which we may disregard commutation noise and vacuum-tube amplifier noise with subsequent amplification of the video signal of a vidicon and for which the signal-to-noise ratio at the vidicon output will be determined only by the signal-to-noise ratio in the incident luminous flux, must be of the order of 500, which is achieved with the wholly realistic value of $\tau_T = 10^{-8}$ sec, $u = 1000$ cm²/v·sec, $\delta = 10^{-4}$ cm, $h = 2$, and γ - 1.

Calculation of Longitudinal-Effect Photocells, I. I. Taubkin and A. I. Frimer, pp. 1120–1129.

The report presents calculation of the inversion characteristics of longitudinal effect photocells in the small-signal case for an arbitrary load in the external longitudinal circuit and arbitrary level of uniform background illumination, as well as in the large-signal case for the open-circuited and short-circuited configurations. The results of calculation may be applied to inversion photocells using germanium, silicon, and other semiconductor materials.

Conclusions: Wallmark's conclusions concerning linearity of the inversion characteristic, being the result of a partial numerical approximation, are not substantiated. A general examination of this case shows that the approximation assumed in another paper is equivalent to nonsteady-state operation of the photocell. On the basis of a more rigorous calculation, expressions have been derived for the inversion characteristics of longitudinal effect photocells in the small-signal case with arbitrary load in the external longitudinal circuit, as well as in the large-signal case for the open-circuited and short-circuited configurations. It is shown that for a low signal level the dependences of longitudinal photovoltages and current for small values of $\alpha_0 l$ are given as straight lines.

The presence of background illumination leads to an increase in parameter α $[\alpha = \alpha_0\sqrt{1 + (j_f/j_s)}]$ and, consequently, to distortion of the linearity of the inversion characteristics and a decrease in longitudinal photosignals.

Number 8, August 1962

Determination of the Concentration of Electrons in the Ionosphere by Analysis of the Polarization Fading in Signals from a Rocket or an Artificial Earth Satellite, S. A. Namazov, pp. 1233–1238.

The rotation of the plane of polarization of radio waves emitted by the transmitter of an artificial satellite or rocket is considered. A method is discussed for obtaining the electron concentration in an observed interval of altitude by the polarization fading in signals from the transmitter of a rocket or satellite. A possible principle for constructing an apparatus for measuring the frequency of the polarization fading is suggested.

Efficient Design of Band Filters with Small Dissipative Losses, S. Kh. Kogan, pp. 1238–1244.

Special Cases of Application of the Fokker-Planck-Kolmogorov Equation, V. I. Tikhonov, pp. 1361–1364.

Passage of Random Signals through a System with Variable Parameters, G. I. Rozhkova and V. S. Etkin, pp. 1364–1366.

In another paper an investigation was made of the problem of the passage of a weak random signal with carrier frequency ω through a nonlinear line, excited simultaneously by a periodic signal of frequency 2ω. It was shown that the phase of the weak output signal may be found only in one of the two rather narrow regions, located π apart, whereby under the specific conditions the relative times that the phase remains in these regions are determined solely by its statistical characteristics at the input of the line. On this basis a conclusion was drawn concerning the possibility of application of a similar system as a phase filter, in which the criterion of the existence of the signal is the variation of the relative time of the output phase existing in one of the possible states.

A comparison of the proposed system with the simplest circuit with variable parameters reveals a complete analogy in their action on a weak random signal. Thus, the input signal and the increase of the percentage modulation of the parameter in the circuit are compared with the boundary condition and the progress along the line (accompanied by an increase of amplitude of the signal).

RUSSIAN JOURNAL OF PHYSICAL CHEMISTRY (*Zhurnal Fizicheskoi Khimii*). Published by The Chemical Society, London

Number 2, 1962

Frozen Radicals and a Higher Peroxide of Hydrogen. VI. Magnetic Properties of Peroxide—Radical Condensates, I. I. Skorokhodov, L. I. Nekrasov, N. I. Kobozev, and V. B. Evdokimov, pp. 136–140.

The previous systematic investigation of peroxide-radical condensates obtained by different methods has shown that they are complicated systems containing, in addition to water and hydrogen peroxide, a higher peroxide of hydrogen (H_2O_4) and frozen HO_2 radicals. The results have enabled us to determine the heat of formation of the compound H_2O_4 from the elements, its heat of decomposition into H_2O_2 and O_2, and also the activation energy of the latter reaction. The presence of HO_2 radicals in peroxide-radical condensates has been observed directly by the electron-paramagnetic-resonance method.

However, in spite of all the data obtained, it has not proved possible to establish the structure of the H_2O_4 molecule. An attempt may be made to obtain some information on this point by a magnetic method. We have therefore measured the magnetic susceptibility of the peroxide-radical condensate both before and during decomposition.

Summary:

1) A study has been made of the magnetic properties between $-150°$ and $20°$ of peroxide–radical condensates prepared both from dissociated water vapor and by reaction of atomic hydrogen with liquid 100% ozone.

2) Before the start of decomposition (below $-110°$) peroxide-radical condensates represent feebly diamagnetic systems with a susceptibility of $-(0.1\text{–}0.2) \times 10^{-6}$ emu. As the temperature rises, an increase in paramagnetism is observed, associated with the appearance in the tube of oxygen evolved by decomposition of the peroxide-radical condensate.

3) The results show that the molecular oxygen evolved on decomposition is not at present adsorbed or occluded in the condensates but is formed by decomposition of the unstable compound H_2O_4, a higher peroxide of hydrogen.

4) The magnetic susceptibility of the compound H_2O_4 has been estimated as 0 to -0.4×10^{-6} emu, which indicates that the valences in this compound are saturated and that it evidently has a chain structure:

$$H\text{—}O\text{—}O\text{—}O\text{—}O\text{—}H$$

Nomogram for Calculating the Composition of Liquid Filters Having a Specified Transmission Maximum in the Visible Spectrum, D. P. Shcherbov, pp. 177–180.

Narrow-band light filters having any specified transmission maximum in the visible region of the spectrum can be prepared by combining two colored solutions of inorganic substances, and are easily accessible. The chief substances selected here are usually available in chemical laboratories and, in contrast to organic dyes, readily yield reproducible spectroscopic properties on simple recrystallization of the original salts. Cells for liquid light filters are easily made of Perspex or from glass for photographic plates, glued together with glyptal.

Summary: A nomogram is proposed for calculating the composition of narrow-band liquid light filters composed of two solutions of colored inorganic substances. The nomogram enables light filters to be prepared with a specified transmission maximum in any part of the visible spectrum, and the absorption limits and spectral width of these light filters to be calculated. The discrepancies between experimental and calculated values do not usually exceed 3–5 mμ.

Number 3, 1962

Emmision Spectrum during Detonation of a Solid Explosive in a Vacuum, V. A. Dement'ev and V. N. Kologrivov, pp. 240–242.

Apart from the work of Alentsev et al. there are no data in the literature on the energy spectrum during detonation of explosives. Investigation of such spectra may provide information on the physical and chemical processes in the reaction zone and on the temperature of the material during detonation. It is also important in connection with experimental techniques, since it may permit appropriate parts of the spectrum to be selected for temperature measurement by brightness, color, or other methods.

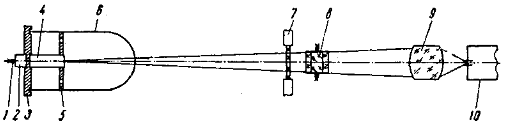

Fig. 1 Diagram of the apparatus: 1) detonating capsule; 2) tablet of TG 50/50; 3) lid; 4) charge; 5) supporting ring; 6) flask; 7) light source; 8) explosion-resistant diaphragm; 9) lens; 10) spectrograph.

In such experiments serious difficulties arise due to the high rate of the process and due to the shock wave formed on detonation in air, since its temperature is higher than that of the detonating charge itself. On the suggestion of M. A. Sadovskii, Corresponding Member of the USSR Academy of Sciences, we undertook experiments on the detonation of explosives in air under reduced pressure, where the air shock wave does not interfere with the observation of the glow of the detonating charge. Photographs obtained on an SFR photorecorder showed that when the detonation wave leaves the end-face of the charge in a vacuum there is a momentary glow, lasting approximately 1 μsec. The spectral range of such glow for charges of TG 50/50 was investigated in the present work.

Formation of Ozone from Dissociation Products of Carbon Dioxide in a Glow Discharge, I. V. Nikitin and E. N. Eremin, pp. 320–323.

Ozone is usually obtained from oxygen at pressures close to atmospheric in a barrier discharge, i.e., in a discharge effected with the aid of one or two dielectric (most often glass) barriers. An instrument of this sort is usually called an ozonizer, and has been the subject of numerous investigations, in particular by Filippov together with Yu. M. Emel'yanov, V. P. Vendillo, Yu.

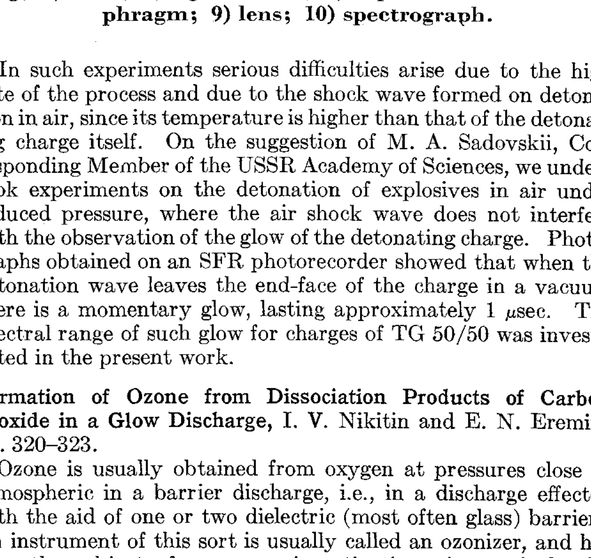

Fig. 1 Diagram of the apparatus for the synthesis of ozone in a glow discharge: 1) manostat; 2, 4, 7, 8, 10, 16, 19, and 22) taps; 3) flow meter; 5) columns; 6) manometer; 12) discharge tube; 13, 17, and 20) traps; 14, 18, and 21) Dewar vessels; 15) LT-2 thermocouple gage; 23) absorber with KI solution.